

# THE METAGALACTIC IONIZING RADIATION FIELD AT LOW REDSHIFT

J. MICHAEL SHULL<sup>1</sup>, DAVID ROBERTS<sup>2</sup>, MARK L. GIROUX,  
STEVEN V. PENTON, AND MARK A. FARDAL<sup>3</sup>  
Center for Astrophysics and Space Astronomy,  
Department of Astrophysical and Planetary Sciences,  
University of Colorado, Campus Box 389, Boulder, CO 80309  
(mshull,giroux,spenton)@casa.colorado.edu

<sup>1</sup> also at JILA, University of Colorado and National Institute of Standards and Technology

<sup>2</sup> Current address: Physics Department, Cornell University, Ithaca, NY 14853; dcr12@cornell.edu

<sup>3</sup> Current address: Department of Physics & Astronomy, University of Massachusetts, Amherst,  
MA 01003; fardal@weka.phast.umass.edu

## ABSTRACT

We compute the ionizing radiation field at low redshift, arising from Seyferts, QSOs, and starburst galaxies. This calculation combines recent Seyfert luminosity functions, extrapolated ultraviolet fluxes from our IUE-AGN database, and a new intergalactic opacity model based on *Hubble Space Telescope* and *Keck Ly $\alpha$*  absorber surveys. At  $z = 0$  for AGN only, our best estimate for the specific intensity at 1 Ryd is  $I_0 = 1.3_{-0.5}^{+0.8} \times 10^{-23}$  ergs cm<sup>-2</sup> s<sup>-1</sup> Hz<sup>-1</sup> sr<sup>-1</sup>, independent of  $H_0$ ,  $\Omega_0$ , and  $\Lambda$ . The one-sided ionizing photon flux is  $\Phi_{\text{ion}} \approx 3400_{-1300}^{+2100}$  photons cm<sup>-2</sup> s<sup>-1</sup>, and the H I photoionization rate is  $\Gamma_{\text{HI}} = 3.2_{-1.2}^{+2.0} \times 10^{-14}$  s<sup>-1</sup>, for  $\alpha_s = 1.8$ . We also derive  $\Gamma_{\text{HI}}$  for  $z = 0 - 4$ . These error ranges reflect uncertainties in the spectral indexes for the ionizing EUV ( $\alpha_s = 1.8 \pm 0.3$ ) and the optical/UV ( $\alpha_{\text{UV}} = 0.86 \pm 0.05$ ), the IGM opacity model, the range of Seyfert luminosities ( $0.001L_* - 100L_*$ ), and the completeness of the luminosity functions. Our estimate is a factor of three lower than the most stringent upper limits on the ionizing background ( $\Phi_{\text{ion}} < 10^4$  photons cm<sup>-2</sup> s<sup>-1</sup>) obtained from H $\alpha$  observations in external clouds, and it lies within the range implied by other indirect measures. Starburst galaxies with a sufficiently large Lyman continuum escape fraction,  $\langle f_{\text{esc}} \rangle \geq 0.05$ , may provide a comparable background to AGN,  $I_0(z = 0) = 1.1_{-0.7}^{+1.5} \times 10^{-23}$  ergs cm<sup>-2</sup> s<sup>-1</sup> Hz<sup>-1</sup> sr<sup>-1</sup>. An additional component of the ionizing background of this magnitude would violate neither upper limits from H $\alpha$  observations nor the acceptable range from other measurements.

*Subject headings:* intergalactic medium — diffuse radiation — galaxies: Seyfert — galaxies: starburst

## 1. INTRODUCTION

The ionizing background that permeates intergalactic space is of fundamental interest for interpreting QSO absorption lines and interstellar high-latitude clouds. Produced primarily by quasars, Seyfert galaxies, and other active galactic nuclei (AGN), these Lyman-continuum (LyC) photons photoionize the intergalactic medium (IGM), set the neutral hydrogen fraction in the Ly $\alpha$  forest absorbers, and help to determine the ion ratios in metal-line absorbers in QSO spectra. Ionizing radiation may control the rate of evolution of the Ly $\alpha$  absorption lines at  $z < 2$  (Theuns, Leonard, & Efstathiou 1998; Davé et al. 1999), and it may affect the formation rate of dwarf galaxies (Efstathiou 1992; Quinn, Katz, & Efstathiou 1996). The hydrogen photoionization rate,  $\Gamma_{\text{HI}}(z)$ , is an important component of N-body hydrodynamic modeling of the IGM. Because of the large photoionization corrections to the observed H I absorption, the inferred baryon density of the IGM and metal abundance ratios also depend on the intensity and spectrum of this radiation. Within the Milky Way halo, the ionizing background can affect the ionization state of high-velocity clouds located far from sources of stellar radiation (Bland-Hawthorn & Maloney 1999).

The ionizing background intensity at the hydrogen ionization edge ( $h\nu_0 = 13.6$  eV) is denoted  $I_0$ , in  $\text{ergs cm}^{-2} \text{s}^{-1} \text{Hz}^{-1} \text{sr}^{-1}$ , hereafter denoted “UV units” or understood in context. In an optically thin environment, the background spectrum reflects that of the sources, QSOs and Seyfert galaxies, which appear to have steep EUV spectra of the form  $F_\nu \propto (\nu/\nu_0)^{-\alpha_s}$ , with  $\alpha_s = 1.77 \pm 0.15$  from 350–1050 Å (Zheng et al. 1997), or starburst galaxies with  $\alpha_s \approx 1.9 - 2.2$  (Sutherland & Shull 1999). At high redshift, the IGM is optically thick, owing to the numerous Ly $\alpha$  absorbers that ionizing photons must traverse. Thus, the background spectrum is strongly modified by absorption and re-emission (Haardt & Madau 1996; Fardal, Giroux, & Shull 1998, henceforth FGS).

Estimates of  $I_0$  at high redshift are usually obtained from the “proximity effect” (Bajtlik, Duncan, & Ostriker 1988), the observed paucity of Ly $\alpha$  absorbers near the QSO emission redshift. Recent measurements give values of  $I_0 \approx 10^{-21}$  UV units at  $z \approx 3$ :  $I_0 = 1.0_{-0.3}^{+0.5} \times 10^{-21}$  (Cooke, Espey, & Carswell 1997),  $I_0 = (0.5 \pm 0.1) \times 10^{-21}$  (Giallongo et al. 1996), and  $I_0 = 0.75 \times 10^{-21}$  (Scott et al. 1999). At low redshift, the lower comoving density of QSOs and their diminished characteristic luminosities suggest that the metagalactic background is reduced by about a factor of  $10^2$  to  $I_0 \approx 10^{-23}$ . Using an optical QSO luminosity function (cf. Boyle 1993) and an empirical model of IGM opacity (Miralda-Escudé & Ostriker 1990), Madau (1992) estimated that  $I_0 = 6 \times 10^{-24}$  at  $z = 0$ . However, this is an uncertain estimate, which now appears low compared with several local determinations. Theoretical extrapolations of  $I_0$  to low  $z$  are uncertain because they depend sensitively on the assumed AGN luminosity function and on the IGM opacity model (Giallongo, Fontana, & Madau 1997; FGS). As we will show, the low- $z$  IGM opacity appears to be dominated by Ly $\alpha$  absorbers in the range  $14 < \log N_{\text{HI}} < 18$ , for which we are just starting to obtain statistically reliable information from the *Hubble Space Telescope* (HST). A future key project on Ly $\alpha$  absorbers with HST and a Ly $\beta$  survey with the *Far Ultraviolet Spectroscopic Explorer* (FUSE) should be even more enlightening.

Observational estimates of or upper limits on  $I_0$  at low redshift have been made by a variety of techniques, as described in Table 1. These methods include studies of the proximity effect at  $\langle z \rangle \approx 0.5$  (Kulkarni & Fall 1993), edges of H I (21 cm) emission in disk galaxies (Maloney 1993; Dove & Shull 1994a), and limits on H $\alpha$  emission from high-latitude Galactic clouds (Vogel et al. 1995; Tufté, Reynolds, & Haffner 1998) and extragalactic H I clouds (Stocke et al. 1991; Donahue, Aldering, & Stocke 1995). Since all these techniques are based on the integrated flux of LyC radiation, it is convenient to define  $\Phi_{\text{ion}}$  (photons  $\text{cm}^{-2} \text{s}^{-1}$ ), the normally incident photon flux through one side of a plane. For an isotropic, power-law intensity,  $I_\nu = I_0(\nu/\nu_0)^{-\alpha_s}$ , we can relate the integral quantity  $\Phi_{\text{ion}}$  to the specific intensity  $I_0$ :

$$\Phi_{\text{ion}} = 2\pi \int_0^1 \mu d\mu \int_{\nu_0}^\infty \frac{I_\nu}{h\nu} d\nu = \left( \frac{\pi I_0}{h\alpha_s} \right) = (2630 \text{ cm}^{-2} \text{ s}^{-1}) I_{-23} \left( \frac{1.8}{\alpha_s} \right), \quad (1)$$

where  $\mu = \cos \theta$  is the angle relative to the cloud normal and  $I_{-23}$  is the value of  $I_0$  expressed in units of  $10^{-23}$  UV units. Most of the upper limits on  $I_0$  translate into values of  $\Phi_{\text{ion}}$  in the range  $10^4 - 10^5$  photons  $\text{cm}^{-2} \text{s}^{-1}$ . For an assumed EUV spectral index  $\alpha_s \approx 1.8$ , and the approximate form,  $\sigma_\nu \approx \sigma_0(\nu/\nu_0)^{-3}$ , for the H I photoionization cross section, the hydrogen photoionization rate due to this metagalactic intensity is,

$$\Gamma_{\text{HI}} \approx \frac{4\pi I_0 \sigma_0}{h(3 + \alpha_s)} = (2.49 \times 10^{-14} \text{ s}^{-1}) I_{-23} \left( \frac{4.8}{3 + \alpha_s} \right), \quad (2)$$

where  $\sigma_0 = 6.3 \times 10^{-18} \text{ cm}^2$  is the hydrogen photoionization cross section at  $h\nu_0$ .

These H $\alpha$  measurements and limits are improving with better Fabry-Perot techniques (Bland-Hawthorn et al. 1994; Tufté et al. 1998). In addition, we now have more reliable HST measurements of the opacity from the low-redshift Ly $\alpha$  clouds (Weymann et al. 1998; Shull 1997; Penton, Stocke, & Shull 1999). Therefore, better computations of the metagalactic radiation field are timely. In this paper, we compute the contribution of Seyfert galaxies, QSOs, and starburst galaxies to the low-redshift ionizing background using three ingredients: (1) a Seyfert/QSO luminosity function; (2) AGN fluxes at  $\lambda < 912 \text{ \AA}$  from extrapolated IUE spectra; and (3) an improved IGM opacity model, based on recent HST surveys of Ly $\alpha$  clouds at low redshift. In § 2 we describe these ingredients. In § 3 we give the results for  $I_0$  and  $\Phi_{\text{ion}}$  at  $z \approx 0$ , together with error estimates. In § 4 we summarize our results and discuss future work that could improve estimates of  $I_0$ .

## 2. METHODOLOGY

The solution to the cosmological radiative transfer equation (Peebles 1993) for sources with proper specific volume emissivity  $\epsilon(\nu, z)$  (in ergs  $\text{cm}^{-3} \text{s}^{-1} \text{Hz}^{-1}$ ) yields the familiar expression (Bechtold et al. 1987) for the mean specific intensity at observed frequency  $\nu_{\text{obs}}$  as seen by an observer at redshift  $z_{\text{obs}}$ :

$$I_\nu(\nu_{\text{obs}}, z_{\text{obs}}) = \frac{1}{4\pi} \int_{z_{\text{obs}}}^\infty \frac{d\ell}{dz} \frac{(1 + z_{\text{obs}})^3}{(1 + z)^3} \epsilon(\nu, z) \exp(-\tau_{\text{eff}}) dz. \quad (3)$$

Here,  $\nu = \nu_{obs}(1+z)/(1+z_{obs})$  is the frequency of the emitted photon (redshift  $z$ ) observed at frequency  $\nu_{obs}$  (redshift  $z_{obs}$ ),  $d\ell/dz = (c/H_0)(1+z)^{-2}(1+\Omega_0 z)^{-1/2}$  is the line element for a Friedmann cosmology, and  $\tau_{\text{eff}}$  is the effective photoelectric optical depth due to an ensemble of Ly $\alpha$  absorption systems. For Poisson-distributed clouds (Paresce, McKee, & Bowyer 1980),

$$\tau_{\text{eff}}(\nu_{obs}, z_{obs}, z) = \int_{z_{obs}}^z dz' \int_0^\infty \frac{\partial^2 \mathcal{N}}{\partial N_{HI} \partial z'} [1 - \exp(-\tau)] dN_{HI}, \quad (4)$$

where  $\partial^2 \mathcal{N} / \partial N_{HI} \partial z'$  is the bivariate distribution of Ly $\alpha$  absorbers in column density and redshift, and  $\tau = N_{HI} \sigma(\nu)$  is the photoelectric (LyC) optical depth at frequency  $\nu$  due to H, He I, and He II through an individual absorber with column density  $N_{HI}$ . For purposes of assessing the local attenuation length, it is useful (Fardal & Shull 1993) to use the differential form of eq. (4), marking the rate of change of optical depth with redshift,

$$\frac{d\tau_{\text{eff}}}{dz} = \int_0^\infty \frac{\partial^2 \mathcal{N}}{\partial N_{HI} \partial z} [1 - \exp(-\tau)] dN_{HI}. \quad (5)$$

The attenuation length, in redshift units, is given by the reciprocal of  $d\tau_{\text{eff}}/dz$ . At low  $z$ , since  $d\tau_{\text{eff}}/dz \lesssim 1$  at the hydrogen threshold, its frequency dependence is significant, and the attenuation length can extend to  $z \approx 2$ . In the past few years, more sophisticated solutions to the cosmological transfer have been developed (Haardt & Madau 1996; FGS) taking into account cloud emission and self-shielding. Figure 1 illustrates our group’s recent calculation of the ionizing background spectrum, computed in full cosmological radiative transfer with a new IGM opacity model based on high-resolution *Keck* spectra of the Ly $\alpha$  forest and local continua. These models include cloud self-shielding and emission. We have connected this high-redshift opacity model with our new model from HST studies (discussed below) for the low-redshift opacity at a transition redshift  $z = 1.9$ . By redshift  $z = 0$ , the intensity has declined to  $I_0 \approx 1.3 \times 10^{-23}$ , corresponding to  $\Phi_{\text{ion}} \approx 3000$  photons  $\text{cm}^{-2} \text{s}^{-1}$  for sources with  $\alpha_s \approx 2$ .

In the work that follows, we compute  $I_\nu$  using both our detailed cosmological radiative transfer code and an approximate solution to equation (3). In this approximation, we neglect the effects of emission from attenuating absorbers and approximate the opacity with a simple power-law fit that neglects the effects of He absorption. We will discuss the accuracy of this approximation in more detail in § 3. Because the opacity of the IGM is much smaller at low redshift, this more rapid calculation is adequate for estimating the present-day level of radiation just above  $\nu_0$ . The primary ingredients for the computation of  $I_0$  at low redshift are the source emissivity,  $\epsilon(\nu, z)$ , and the opacity model for  $\tau_{\text{eff}}(\nu_{obs}, z_{obs}, z)$ . In the following sub-sections, we describe how we determined these quantities.

## 2.1. AGN Luminosity Function and Spectra

The distribution of AGN luminosities is typically described by a rest-frame, B-band luminosity function. In order to estimate the total emissivity of AGN at the Lyman limit, we must know

both the luminosity function and the average spectrum of the AGN. In addition, we must know the assumptions about the spectrum that were made to construct the luminosity function.

To estimate the intrinsic AGN quasar spectrum, we begin with the Seyfert optical sample of Cheng et al. (1985), based on Seyfert 1 and 1.5 galaxies covered by the first nine Markarian lists. Their sample was corrected for incompleteness, and the contribution from the host galaxy was subtracted out. The separation of nuclear and host galaxy luminosity becomes increasingly challenging at the faint end of the luminosity function. Ideally, careful, small-aperture photometry would be used for these estimates. Cheng et al. (1985) relied instead on two independent methods to separate the contribution from the nucleus. In the first method, they assumed a template host galaxy and corrected this for orientation and internal extinction. In the second method, they assumed that all nuclei had the same intrinsic colors and determined the nuclear contribution via the color-given method of Sandage (1973). They found these two methods to give consistent results. In addition, they compared the color-given method with nuclear magnitudes derived by careful surface photometry for 11 Seyfert 1 galaxies (Yee 1983). They assigned a total uncertainty of 0.5 mag in the nuclear  $M_B$  to the sample. On re-examination of the sample, we found that the errors most likely decrease with the luminosity of the galaxy. We assume that the errors on the specific luminosity,  $L_B$  (ergs s<sup>-1</sup> Hz<sup>-1</sup>), decrease linearly from 0.24 dex at  $\log L_B = 28$  to 0.16 dex at  $\log L_B = 30$ .

From this sample of Seyferts, we chose 27 objects observed repeatedly by the *International Ultraviolet Explorer* (IUE) satellite. Together with many other AGN, these Seyfert galaxies are part of the Colorado IUE-AGN database (Penton, Shull, & Edelson 1996), which gives both mean and median spectra. Since these AGN are subject to flux variability, the distribution in flux is a skewed distribution with a tail that includes short flares studied by various IUE campaigns. To provide a conservative estimate of the ionizing fluxes, we have therefore used median spectra to derive correlations; however the differences in the correlations are only a few percent. The line-free regions of the median IUE spectra were fitted to power-law continua and extrapolated to 912 Å (rest-frame), from which we derive the specific luminosity,  $L_{912}$  (ergs s<sup>-1</sup> Hz<sup>-1</sup>). We also convert from  $M_B$  to  $L_B$ , at  $\nu = 6.81 \times 10^{14}$  Hz (4400 Å) by the formula derived from Weedman (1986, eqs. 3.15 and 3.16),  $\log L_B = 0.4(51.79 - M_B)$ . Figure 2 shows the correlation between  $L_{912}$  and  $L_B$ . The error bars are only shown for  $L_B$ , since the errors in  $L_{912}$  are much smaller. We find that  $L_{912} = (2.60 \pm 0.22) \times 10^{28} (L_B/10^{29})^{(1.114 \pm 0.081)}$  erg s<sup>-1</sup> Hz<sup>-1</sup>. This translates to a UV-optical spectral slope that depends on  $L_B$  as

$$\alpha_{UV} = (0.86 \pm 0.05) - (0.16 \pm 0.12) \log(L_B/10^{29}) . \quad (6)$$

The evidence for  $L_B$  dependence is marginal, however, and our basic model will simply assume a constant slope  $\alpha_{UV} = 0.86$  between the B band and the Lyman limit. This agrees quite well with the average QSO spectrum derived by Zheng et al. (1997).

The second ingredient in the computation of the AGN emissivity is the luminosity function. The function that matches observations over the broadest redshift and luminosity range is the

comoving analytic form given by Pei (1995, eqs. 6–8),

$$\Phi(L, z) = \frac{\Phi_*/L_z}{(L/L_z)^{\beta_l} + (L/L_z)^{\beta_h}}, \quad (7)$$

where the characteristic “break luminosity” is given by

$$\begin{aligned} L_z &= L_*(1+z)^{-(1-\alpha_{UV})} \exp\left[-(z-z_*)^2/2\sigma_*^2\right] \\ &= L_0(1+z)^{-(1-\alpha_{UV})} \exp\left[-z(z-2z_*)/2\sigma_*^2\right]. \end{aligned} \quad (8)$$

Here,  $\alpha_{UV}$  is the UV-optical spectral index and  $L_0 = L_* \exp(-z_*^2/2\sigma_*^2)$  is the “break luminosity”,  $L_z$ , at the present epoch. Note that we define our spectral index with the opposite sign to that assumed by Pei, i.e., we adopt  $L_\nu \propto \nu^{-\alpha_{UV}}$  where most data suggest that  $0.5 < \alpha_{UV} < 1$ . We present results for luminosity functions based on the two sets of assumptions about the cosmology and optical spectral index  $\alpha_{UV}$  derived by Pei. The “open model” has  $h = 0.5$ ,  $\Omega_0 = 0.2$ , and  $\alpha_{UV} = 1.0$  and yields  $\beta_l = 1.83$ ,  $\beta_h = 3.70$ ,  $z_* = 2.77$ ,  $\log(L_*/L_\odot) = 13.42$ ,  $\sigma_* = 0.91$ , and  $\log(\Phi_*/\text{Mpc}^{-3}) = -6.63$ . The “closed universe” model has  $h = 0.5$ ,  $\Omega_0 = 1$ , and  $\alpha_{UV} = 0.5$  and yields  $\beta_l = 1.64$ ,  $\beta_h = 3.52$ ,  $z_* = 2.75$ ,  $\log(L_*/L_\odot) = 13.03$ ,  $\sigma_* = 0.93$ , and  $\log(\Phi_*/\text{Mpc}^{-3}) = -6.05$ . Figure 3 shows these two models at  $z = 0$ . After correcting for the different spectral indices, there is no physical reason why these two models should differ in the ionizing intensity they imply or in their value as  $z \rightarrow 0$ . However, the intensity estimates from these models differ by up to 40% (see FGS). This points to substantial uncertainties in the Pei fit that are not reflected in the small formal errors.

We integrate the ionizing luminosity density over the luminosity function from  $L_{\min}$  to  $L_{\max}$ . In our standard model, we assume that these limits are  $0.01L_z$  and  $10L_z$ , respectively, and we explore the sensitivity of the results to  $L_{\min}$ . If we define  $x = L/L_z$ , we can write the comoving specific volume emissivity as

$$\epsilon(\nu, z) = \Phi_* \left(\frac{\nu_0}{\nu_B}\right)^{-\alpha_{UV}} \left(\frac{\nu}{\nu_0}\right)^{-\alpha_s} L_z \int_{x_{\min}}^{x_{\max}} \frac{x}{x^{\beta_l} + x^{\beta_h}} dx, \quad (9)$$

where we assume an EUV power-law spectral index  $\alpha_s$  for the AGN and integrate from  $x_{\min} = L_{\min}/L_z$  to  $x_{\max} = L_{\max}/L_z$ . With  $x_{\min} = 0.01$  and  $x_{\max} = 10$ , our results are insensitive to  $x_{\max}$  and moderately insensitive to  $x_{\min}$ . An increase (decrease) of  $x_{\min}$  by a factor of 3 leads to a decrease (increase) of the calculated emissivity by 15%. A similar change of  $x_{\max}$  changes the emissivity by only 2%. From several trials, we find an empirical scaling relation,  $I_0^{\text{AGN}} \propto (L_{\min}/0.01L_*)^{-0.17}(\alpha_s/1.8)^{-0.97}$ . To better assess the uncertainty from the extrapolation to bright and faint sources, we use Figure 2 of Pei (1995), which shows the range of B luminosities that contribute to the luminosity function fit. We define the “completeness” as the integral of the emissivity over this range, compared with the integral for the standard range  $0.01 < x < 10$ . This completeness rises from 20% at  $z = 0$  to 80% at  $z \sim 2$ , but falls to 20% at  $z \sim 4$ . The low- $z$  results can be made more robust by considering additional surveys of Seyferts and QSOs.

Figure 3 shows the B-magnitude luminosity function from the Cheng et al. (1985) sample, as well as the results from the survey of Köhler et al. (1997) for Seyferts and QSOs with  $z < 3$ . These results are also compatible with the results of the local optical luminosity function based on an X-ray selected sample of AGN (Della Ceca et al. 1996). There are some discrepancies, however, between these results and the Pei luminosity function. There are more QSOs at the bright end of the luminosity function at  $z < 1$  than in the Pei form, an effect that has been noted by several authors (Goldschmidt et al. 1992; Goldschmidt & Miller 1998; La Franca & Cristiani 1997). This appears to have its origin in systematic errors in the Schmidt & Green (1983) QSO survey. In addition, there appears to be a slight deficit at the knee of the Pei function in both the Köhler et al. and Cheng et al. samples. In fact, the Köhler results are fitted adequately with a single power law, as shown in Fig. 3.

It turns out that these two effects cancel to within 5% when we compute the total B-band emissivity over the range  $0.01 < L_B/L_z(0) < 10$ . However, the fact that the luminosity function appears to be changing shape weakens the assumptions leading to the Pei function, and the convergence at the faint end becomes even slower.

Hence, our best estimate of the emissivity is unchanged from the Pei (1995) model, but we suspect that there are still substantial uncertainties in the AGN luminosity function. In Fig. 4 we plot the emissivity from the Pei “open” model. To find a reasonable range of emissivity models, we multiply (or divide) this by the square root of the “completeness” of the Pei model as derived above, and we also change the spectral slope  $\alpha_{UV}$  and its dependence on  $L_B$  by one standard deviation to minimize (or maximize) the ionizing emissivity. We consider the band thus defined to be a conservative  $1\sigma$  range for the emissivity. Note that the Pei “closed” model, adjusted for the different spectral index and cosmology, lies well within this range.

The average UV QSO spectrum derived by Zheng et al. (1997) implies an EUV spectral index  $\alpha_s = 1.77 \pm 0.15$  for radio-quiet QSOs and  $\alpha_s = 2.16 \pm 0.15$  for radio-loud quasars. Since radio-quiet QSOs are much more numerous, we select  $\alpha_s = 1.8 \pm 0.15$  as a representative measure of the EUV spectral index.

## 2.2. Stellar Contributions to the Ionizing Emissivity

The contribution of stars within galaxies to the ionizing background remains almost completely unknown at all epochs. It has been realized (cf. Madau & Shull 1996) that the amount of ionizing photons associated with the production via supernovae of the observed amount of metals in the universe might easily exceed the ionizing photons produced by AGNs. The problem has been to estimate the average fraction,  $\langle f_{esc} \rangle$ , of ionizing photons produced by O and B stars that escape the galaxies into the IGM. Thus far, observational limits on  $\langle f_{esc} \rangle$  exist from only a few nearby galaxies (Leitherer et al. 1995; Hurwitz et al. 1997). On theoretical grounds, Dove & Shull (1994b) concluded that an escape fraction of order 10% might be possible, while more recent

models of the escape of ionizing photons through supershell chimneys (Dove, Shull, & Ferrara 1999) suggest fractions of 3–6%, which are compatible with the observational limits. Recently, Bland-Hawthorn & Maloney (1999) used measurements of H $\alpha$  from the Magellanic Stream to infer an escape fraction  $\sim 6\%$  from the Milky Way.

Deharveng et al. (1997) argued that even the present indirect upper limits on  $I_0$  must limit the present-day escape fraction to below 1%. They depart radically, however, from the work of Dove & Shull (1994b) and Dove et al. (1999) in their treatment of the nature of the escape fraction. Deharveng et al. assume that stellar ionizing photons are prevented from escaping their host galaxies by the opacity of neutral hydrogen, effectively in the limit that the hydrogen forms an unbroken sheet. Consequently, the opacity varies approximately as  $(\nu/\nu_0)^{-3}$ , so that the escape of higher-energy photons is dramatically enhanced. For example, the optical depth can decrease from  $\tau \approx 50$  at the Lyman edge to  $\tau < 1$  at 4 rydbergs. For photons emitted at high redshift that survive to contribute to  $I_0$  at  $z = 0$ , the sharp increase in the escape fraction outweighs the effects of redshifting. In the Deharveng picture, the contribution of high- $z$  galaxies to the present-day mean intensity at  $\nu = \nu_0$  is strongly enhanced. Thus, if  $\langle f_{esc} \rangle \approx 0.001$ , starbursts may match the contribution of quasars to the present-day ionizing mean intensity.

However, we believe the Deharveng model for photon escape is physically unrealistic. Our alternative view is that the internal galactic opacity to all stellar photons is large, and photons may only escape from isolated regions of high star formation whose H II regions or attendant supershells are able to break through this high opacity layer (Dove et al. 1999). Within this view, a constant escape fraction with frequency is more appropriate.

Our estimate of the stellar ionizing photons is made in the following way. Gallego et al. (1995) performed an H $\alpha$  survey of galaxies and fitted their derived luminosity function to a Schechter function. By integrating this, they were able to estimate a total H $\alpha$  luminosity per unit volume at low redshift,  $L_{H\alpha} = 10^{39.1 \pm 0.2}$  erg s $^{-1}$  Mpc $^{-3}$ . In the usual fashion, we relate this to the number of ionizing photons by dividing the number of H $\alpha$  photons by the fraction of the total H recombinations that produce an H $\alpha$  photon. We multiply their estimate of the ionizing photon production by  $\langle f_{esc} \rangle$  to give the total ionizing photons in the IGM. The representative models assume  $\langle f_{esc} \rangle = 0.05$  and are shown in Figure 5. Preliminary results are now available from the KPNO International Spectroscopic Survey (KISS) (Gronwall et al. 1998), which probes to fainter magnitudes than the Gallego et al. survey. Gronwall (1998) quotes a value  $L_{H\alpha} = 10^{39.03}$  erg s $^{-1}$  Mpc $^{-3}$ , but notes that these results are preliminary and represent a lower limit to the true H $\alpha$  density, since even their deeper survey is incomplete for galaxies with H $\alpha$  emission-line equivalent widths less than 25 Å.

The spectrum of ionizing photons from clusters of hot stars differs from that of AGN in that stars emit relatively few photons more energetic than 4 Ryd. Sutherland & Shull (1999) have shown that, between 1 and 4 Ryd, the spectrum of a starburst may be approximated as a power law with spectral index  $\alpha_s = 1.9 - 2.2$ .



We have tied the redshift evolution in ionizing photon production rate to the star formation evolution observations of Connolly et al. (1997) based upon the Hubble Deep Field (HDF). The effects of dust extinction remain a major uncertainty in the determination of the star formation rate at high redshift (cf. Pettini et al. 1998). Many high- $z$  star-forming galaxies appear to be dust-obscured, based on recent sub-millimeter studies of the HDF (Hughes et al. 1998; Barger et al. 1998). In addition, a survey of Lyman-break galaxies at  $z \approx 3 - 4$  (Steidel et al. 1999), covering a much larger angular extent than the HDF, finds no significant difference in the star formation rate at  $z = 3$  and  $z = 4$ . With corrections for dust extinction, the star formation could remain constant from  $z = 1.5$  out to  $z > 4$ . As a result, we have also considered a case in which the star formation remains constant after reaching its peak at  $z \approx 2$ . However, despite the many uncertainties of high- $z$  star formation rates, the effects on the present-day level of ionization are minimal, of order a few percent.

### 2.3. Absorption Model for the IGM

At  $z < 2$ , the redshift densities of the Ly $\alpha$  clouds and Lyman limit systems decline steeply with cosmic time. Morris et al. (1991) and Bahcall et al. (1991) used HST observations to show that this decline could not be extrapolated to the present, as far too many Ly $\alpha$  absorbers were observed toward 3C 273. The large data set gathered by the Hubble Key Project with the Faint Object Spectrograph (FOS) shows a sharp break in the evolving redshift density at  $z \sim 1.5 - 2$  (Weymann et al. 1998). Ikeuchi & Turner (1991) showed that the cessation in this steep decline was a natural consequence of the falloff in the ionizing emissivity from  $z = 2$  down to 0. This conclusion has been borne out by detailed cosmological simulations (Davé et al. 1999), which indicate that the effect is insensitive to the specific cosmological model.

In our calculations, we will base our absorption model on observations. Our analysis follows the traditional “line-counting” method, where spectral lines are identified by Voigt profile-fitting and the opacity is calculated by assuming a Poisson distribution of these lines. At high redshift, FGS used this method to estimate the opacity based on high-resolution observations of QSO Ly $\alpha$  absorption lines from *Keck* and other large-aperture telescopes in the redshift range  $2 \leq z \leq 4$ . It is not appropriate to extrapolate this model to lower redshifts, owing to the rapid evolution rate of the Ly $\alpha$  forest.

Our method of determining  $d\tau_{\text{eff}}/dz$  considers Ly $\alpha$  lines in three ranges of column density: from  $12.5 < \log N_{HI} < 14.0$  (HST/GHRS survey), from  $14.0 < \log N_{HI} < 16$  (HST/FOS survey), and for  $\log N_{HI} > 17$  (HST/FOS Lyman-limit survey). The HST/FOS survey forms the core of our standard opacity model. We combine these results with HST/GHRS measurements of weak lines and with the HST/FOS survey of Lyman-limit systems, extrapolated downward from the Lyman limit by two different methods. At redshifts  $z < 1.5$ , the most extensive study of strong Ly $\alpha$  absorbers ( $10^{14-16} \text{ cm}^{-2}$ ) is the QSO Absorption Line Key Project with HST/FOS (Januzzi et al. 1998; Weymann et al. 1998). Weaker Ly $\alpha$  lines, which contribute a small amount

to the opacity and serve as a constraint on the column density distribution, were studied by Shull (1997), Shull, Penton, & Stocke (1999), and Penton et al. (1999) using HST/GHRS spectra. The distribution of Lyman limit systems with  $N_{HI} > 10^{17} \text{ cm}^{-2}$  are discussed by Stengler-Larrea et al. (1995) and Storrie-Lombardi et al. (1994). Each of these surveys suffers from incompleteness or saturation effects in various regimes. Therefore, extrapolations outside the range of  $N_{HI}$  and comparisons in regimes of overlap are helpful. Extensive future UV surveys with HST and FUSE will also reduce some of the uncertainties (see discussion in § 4).

HST/GHRS studies of Ly $\alpha$  absorbers in the range  $12.5 \leq \log N_{HI} \leq 14.0$  (Penton et al. (1999) find a column density distribution,  $d\mathcal{N}/dN_{HI} \propto N_{HI}^{-1.74 \pm 0.26}$ . The cumulative opacity of these weak lines (up to  $10^{14} \text{ cm}^{-2}$ ) is relatively small:  $d\tau_{\text{eff}}/dz = 0.025 \pm 0.005$  for the low-redshift range ( $0.003 < z < 0.07$ ). However, a small number of higher column density systems produce a steady rise in the cumulative opacity for  $\log N_{HI} > 14$ . Extending the HST/GHRS distribution up to  $\log N_{HI} = 15$  gives  $d\tau_{\text{eff}}/dz \approx 0.09 \pm 0.02$ . Above this column density, saturation effects and small-number statistics make the number counts more imprecise. In the range  $15 < \log N_{HI} < 16$ , Penton et al. (1999) estimate an additional contribution,  $d\tau_{\text{eff}}/dz \approx 0.1 - 0.3$ .

The HST/FOS Key Project spectra have insufficient resolution to determine line widths or to resolve velocity components. As a result, the conversion from equivalent width,  $W_\lambda$ , to column density,  $N_{HI}$ , is difficult for saturated lines. In the absence of other lines (e.g., Ly $\beta$ ), one can only estimate the conversion from  $W_\lambda$  to  $N_{HI}$  by assuming a curve of growth and doppler parameter. This difficulty was noted by Hurwitz et al. (1998) in their comparison of unexpectedly strong ORFEUS Ly $\beta$  absorption compared to predictions from HST Ly $\alpha$  lines toward 3C 273. For unsaturated lines,  $W_\lambda = (54.4 \text{ m}\text{\AA})N_{13}$ , where  $N_{HI} = (10^{13} \text{ cm}^{-2})N_{13}$  and where the line-center optical depth is  $\tau_0 = (0.303)N_{13}b_{25}^{-1}$  for a doppler parameter  $b = (25 \text{ km s}^{-1})b_{25}$ . The HST/FOS Key Project lines with  $W_\lambda \geq 240 \text{ m}\text{\AA}$  are highly saturated in the range ( $14 \leq \log N_{HI} \leq 17$ ) that dominates the Ly $\alpha$  forest’s contribution to the continuum opacity.

As a first attempt to incorporate the Key Project information, we focus on the statistical frequency of Ly $\alpha$  absorbers,  $d\mathcal{N}/dz = 30.7 \pm 4.2$ , for lines with  $W_\lambda > 240 \text{ m}\text{\AA}$ . For  $b = 25 \text{ km s}^{-1}$ , this corresponds roughly to  $\log N_{HI} > 14$ . We compute opacities based upon sample 5 of Weymann et al. (1998), which includes 465 absorption lines ( $W_\lambda > 240 \text{ m}\text{\AA}$ ) that could not be matched with corresponding metal lines. This sample was intended to remove high column density lines that may evolve more rapidly with redshift, consistent with the results of Stengler-Larrea et al. (1995) for Lyman limit systems. This segregation has little effect on the opacity. The Key Project became incomplete at column densities well below the Lyman limit. Therefore, to determine an IGM opacity, we needed to extrapolate to  $\log N_{HI} = 17$  using assumptions about the distribution.

The bivariate distribution of Ly $\alpha$  absorbers per unit redshift and unit column density can be expressed as  $\partial^2\mathcal{N}/\partial z \partial N_{HI} = A(N_{HI}/10^{17} \text{ cm}^{-2})^{-\beta}(1+z)^\gamma$ . Improvements on this form have been suggested, notably the addition of one or more breaks in the power-law distribution (Petitjean et al. 1993; FGS). Here, we parameterize our uncertainty by assuming just one power-law index,

but we vary the upper limit on column density to which we integrate. Figure 6 shows a set of curves, corresponding to  $\beta = 1.5 \pm 0.2$ , of the differential effective opacity,  $d\tau_{\text{eff}}/dz$ , evaluated at  $z = 0$  and at the hydrogen threshold. Assuming  $\beta = 1.5$  and no break in the distribution, we find  $d\tau_{\text{eff}}/dz \approx 0.2$  for the FOS range  $10^{14-16} \text{ cm}^{-2}$  and  $d\tau_{\text{eff}}/dz \approx 0.5$  for the expanded range  $10^{14-17} \text{ cm}^{-2}$ . Because  $\gamma = 0.15 \pm 0.23$  for this FOS sample, the opacity does not change greatly with redshift. We choose a standard value  $d\tau_{\text{eff}}/dz \approx 0.5$ , corresponding to  $\beta = 1.5$  and  $N_{\text{max}} = 10^{17} \text{ cm}^{-2}$ .

The Lyman-limit data (Stengler-Larrea et al. 1995) can be fitted to the form

$$\frac{d\tau_{\text{eff}}}{dz} = 0.263(1+z)^{1.50}, \quad (10)$$

assuming that  $\partial^2 \mathcal{N} / \partial z \partial N_{HI} \propto N_{HI}^{-1.5} (1+z)^{1.50}$ . In absorption model 1, we took the lower limit on  $N_{HI}$  for partial LL systems to be  $N_l = 10^{17} \text{ cm}^{-2}$ . If this limit is extended down to  $10^{16} \text{ cm}^{-2}$  or  $10^{15.5} \text{ cm}^{-2}$ , the coefficient 0.263 in eq. (10) increases to 0.382 and 0.411, respectively; the latter choice becomes our Model 2.

We summarize our three opacity models in Table 2. We use equation (5) to calculate the opacity, but include an approximation of the frequency dependence of the opacity over the range 1–3 Ryd, which dominates the H I photoionization rate. This approximation takes the form

$$\frac{d\tau_{\text{eff}}}{dz} = c_i \left( \frac{\nu}{\nu_0} \right)^{s_i} (1+z)^{\gamma_i}. \quad (11)$$

In Figure 7, we compare  $d\tau_{\text{eff}}/dz$  at  $\nu = \nu_0$  for the three models described above, as well as low-redshift extrapolations of the opacities of FGS and Haardt & Madau (1996). It can be seen that the poorly determined column-density distribution of the Ly $\alpha$  forest leaves a large uncertainty in the total opacity, even though the evolution of the number density is tightly constrained by the HST observations. The partial LL systems ( $16 \leq \log N_{HI} \leq 17.5$ ) probably dominate the IGM opacity at low redshift, but they are so rare that statistical fluctuations from sightline to sightline are quite large. It will require many high signal-to-noise spectra along low redshift lines of sight to reduce the uncertainty in their contribution to the opacity.

### 3. RESULTS: THE IONIZING RADIATION FIELD

#### 3.1. The Contribution from AGN

Our best-estimate model for the present day intensity  $I_0$  makes the following four assumptions: (1) The AGN distribution is described by the Pei (1995) QSO luminosity function with  $h = 0.5$  and  $\Omega_0 = 0.2$ , modified by the assumption that the optical-UV spectral index  $\alpha_{UV} = 0.86$ , but with no correction for intervening dust. (2) The lower (upper) cutoffs to the luminosity function are  $L_{\text{min(max)}} = 0.01(10)L_*$ . (3) The opacity below  $z \approx 1.9$  is our “standard model,” itself based upon HST observations of Ly $\alpha$  forest and Lyman Limit systems. Above  $z \approx 1.9$ , it is Model A2

from FGS. (4) The ionizing spectrum ( $\nu \geq \nu_0$ ) has spectral index  $\alpha_s = 1.8$ . Using the full radiative transfer calculation outlined in FGS, we find

$$I_0 = 1.3_{-0.5}^{+0.8} \times 10^{-23} \text{ erg cm}^{-2} \text{ s}^{-1} \text{ Hz}^{-1} \text{ sr}^{-1}. \quad (12)$$

As we discuss below, most of the uncertainties in our estimate are essentially multiplicative. The uncertainties quoted above represent the addition in quadrature of the uncertainties in the log of the factors discussed below. Direct addition in quadrature of the relative uncertainties gives a similar range of uncertainty. Strictly speaking, although none of the uncertainties is independent, we treat them as if they were in computing the total uncertainty.

Figure 4 summarizes the uncertainties in the emissivity due to AGN that pertain to assumptions (1) and (2). The corresponding  $1 \sigma$  uncertainty in the calculated specific intensity for the  $\Omega_0 = 0.2$  case is  $\pm 0.19$  dex. As FGS noted, the intensity should be independent of the choice of  $H_0$  or  $\Omega_0$  if the emissivity is actually determined observationally. The AGN luminosity function is propagated from low to high redshift, assuming pure luminosity evolution, a parameterization that depends only on  $z$ , and not explicitly on appropriate cosmological distances and luminosity evolution parameters. The difference in the calculated mean intensity for a closed universe ( $\Omega_0 = 1$ ) is not an independent source of uncertainty. However, we estimate an uncertainty of  $\pm 0.01$  dex, which is negligible.

The uncertainties inherent in our choice of opacity model appear both in the degree of attenuation of ionizing photons due to the absorbers, and in the contribution of diffuse ionizing radiation from the absorbers (mainly He II ionizing photons reprocessed to He II Ly $\alpha$  and two-photon radiation). Using Models 1 and 2 instead of our standard model, we calculate slightly higher levels of  $I_0$ , by factors of 0.0068 and 0.0329 dex. A sample standard deviation of the models is  $\pm 0.017$  dex and is probably an adequate assessment of the  $1\sigma$  uncertainty in  $I_0$  due to the opacity. A more complete picture of the full (at least several  $\sigma$ ) uncertainty may be obtained from the following extreme cases. The diffuse ionizing radiation from absorbers contributes 20% of the ionizing intensity at  $z = 0$  (see Fig. 8a), so eliminating this contribution reduces  $I_0$  by 0.1 dex. If there is no opacity at all,  $I_0$  increases by 0.26 dex. If the column density distribution for the absorbers in our standard model is assumed have an unbroken power law with  $\beta = 1.3$  rather than 1.5, the reduction in  $I_0$  is 0.21 dex. The shape of the spectrum of AGN shortward of 912 Å is a relatively small source of uncertainty. As  $\alpha_s$  is varied between 1.5 and 2.1, representative of the  $2 \sigma$  uncertainty in  $\alpha_s$ , the relative specific intensity varies by  $\pm 0.1$  about the standard value  $\alpha_s = 1.8$ . We therefore adopt a conservative uncertainty of  $\pm 0.1$  dex in  $I_0$ .

There remains an additional systematic uncertainty in the contribution of AGN to  $I_0$ . As discussed by FGS, the Pei luminosity function used here produces insufficient ionizing photons to account for the level of the ionizing background at  $z > 3.5$  implied by the proximity effect. Further, there are not enough ionizing photons to reionize the universe by  $z \approx 5$  (Madau 1998), the epoch of the highest redshift quasars. While the latter point remains a problem for scenarios in which only AGN ionize the IGM, the former difficulty is ameliorated by the suggestion that,

especially at higher redshifts, the number of AGN are being undercounted due to obscuration by dust-laden absorbers (Heisler & Ostriker 1988; Fall & Pei 1993; Pei 1995). Using the dust-corrected luminosity function of Pei (1995), we find that  $I_0$  at  $z = 0$  is increased by 0.08 dex.

As shown in Fig. 1, the level of the mean intensity at  $z \approx 2$  calculated by FGS is  $I_0 \approx 7 \times 10^{-22}$ . For this model, ionizing radiation due to sources at  $z > 2$  produces 20% of the mean intensity at  $z = 0$  (see Fig. 8a). As Fig. 1 shows, redshifted He II Ly $\alpha$  diffuse emission is still substantial at  $z = 2$ . Because He II  $\lambda 304$  emitted at  $z > 2$  is redshifted below the H I threshold by  $z = 0$ , this emission contributes less than 10% at  $z = 0$ . To give a specific example, suppose that the number of AGN at high redshift was severely underestimated, so that the metagalactic background due to AGN at  $z \approx 2 - 3$  was quintupled, while retaining the same spectral shape. Then, the value of  $I_0$  at  $z = 0$  would be increased by only 0.15 dex. Even for AGN, the strong attenuation of high-energy photons by He II absorption greatly limits any contribution to the present-day ionizing background from sources at  $z > 3$ . A significantly larger population of AGN at  $z = 2 - 3$  will not augment  $I_0$  by more than 40% at  $z = 0$ . This systematic effect has not been included in the uncertainty in eq. (12).

### 3.2. The Possible Contribution from Hot Stars

An estimate of the ionizing radiation contributed by hot stars is complicated by its dependence on factors such as  $\langle f_{esc} \rangle$ , for which a good estimate of its magnitude and uncertainty does not exist. As a result, we include these factors explicitly in our results. Our model for the possible contribution of stars to the present day specific intensity  $I_0$  makes the following assumptions: (1) The production of ionizing photons by stars at the present time may be calibrated by the density of H $\alpha$  photons in the extragalactic background. (2) The star formation rate is proportional to that from the observations of Connolly et al. (1997) and assumes  $h = 0.5$  and  $\Omega_0 = 0.2$ . (3) The IGM opacity is our “standard model.” (4) The average spectrum of the OB associations that provide the ionizing photons has spectral index  $\alpha_s = 1.9$  (1 – 4 Ryd) with no photons above 4 Ryd. Using a radiative transfer calculation that neglects the diffuse radiation contributed by intervening absorbers (see discussion below), we find

$$I_0 = 1.1_{-0.7}^{+1.4} \times 10^{-23} \left( \frac{\langle f_{esc} \rangle}{0.05} \right) \left( \frac{L_{H\alpha}}{10^{39.1}} \right) \text{ erg cm}^{-2} \text{ s}^{-1} \text{ Hz}^{-1} \text{ sr}^{-1}, \quad (13)$$

where we have scaled the H $\alpha$  luminosity density,  $L_{H\alpha}$ , to the Gallego et al. (1995) standard value,  $10^{39.1} \text{ erg s}^{-1} \text{ Mpc}^{-3}$ , and adopted a probable LyC escape fraction,  $\langle f_{esc} \rangle = 0.05$ .

The uncertainties for which we have not directly parameterized our ignorance are mainly multiplicative, as in the case for AGN. The uncertainty in the numerical coefficient quoted above again represents the addition in quadrature of the uncertainties in the log of the factors discussed below. We make the same conservative assumption that the individual uncertainties are independent. The uncertainty in the H $\alpha$  luminosity density suggested by Gallego et al. (1995)

is  $\pm 0.2$  dex, while the uncertainty in the preliminary KISS result, is  $\pm 0.1$  dex. We adopt an uncertainty of  $\pm 0.2$  dex for the  $H\alpha$  calibration, but it is possible that this uncertainty will be reduced substantially when full details of KISS are released. As long as  $\langle f_{esc} \rangle$  is small, so that recombinations within the galaxies provide a fair accounting of the number of ionizing photons produced, this is the uncertainty we associate with assumption (1). The conversion of  $H\alpha$  photons to ionizing photons is nearly temperature independent, so uncertainties in the temperature of ionized regions in galaxies are negligible. The  $H\alpha$  emissivity is parameterized directly in units of the luminosity density suggested by Gallego et al. (1995), but the uncertainty discussed above is included in the numerical coefficient.

The uncertainties in the stellar emissivity (assumption 2) are summarized in Fig. 5. The error bars in the points from the Connolly et al. data are formulated in a different way from our evaluation of the AGN uncertainty. These authors corrected for survey incompleteness using a Schechter function with three different power laws to extrapolate to low luminosity. We show a rough  $1\sigma$  range in the emissivity based upon this estimate of the uncertainties. Our emissivity depends upon a fit to the data points in Fig. 5, and has small variations with the assumed cosmology. This introduces a small uncertainty of 0.01 dex in the calculation of  $I_0$ .

The uncertainty inherent in our choice of opacity model, assumption (3) above, appears primarily in the degree of IGM attenuation of ionizing photons. If we focus only on the stellar contribution to the ionizing background, the number of He II ionizing photons produced is negligible. As a result, the contribution of diffuse ionizing radiation from the absorbers may be neglected. (Because H I recombination radiation is closely confined to the ionization edge, this diffuse radiation is quickly redshifted below  $\nu_0$ .) Using Models 1 and 2 for the opacity instead of our standard model, we calculate slightly higher levels of  $I_0$ , by factors of 0.0068 and 0.0329 dex. A sample standard deviation of the models is  $\pm 0.017$  dex and is probably an adequate assessment of the  $1\sigma$  uncertainty in  $I_0$  due to the opacity. If there is no opacity at all,  $I_0$  increases by 0.26 dex. If the column density distribution for the absorbers in our standard model has an unbroken power law, with  $\beta = 1.3$  rather than 1.5, the reduction in  $I_0$  is 0.21 dex.

Our assumption (4), that the stellar ionizing radiation has a spectrum  $\nu^{-1.9\pm 0.2}$  (Sutherland & Shull 1999), yields a relatively small source of uncertainty. As  $\alpha_s$  is varied between 1.7 – 2.1, the specific intensity increases by factors of 0.045 to  $-0.043$  dex. We therefore assign an uncertainty of  $\pm 0.045$  dex.

As shown in Fig. 8b, the contribution from stars at  $z > 2$  to the present ionizing radiation background just above the Lyman edge is less than 3%. This assumes that the emissivity peaked at  $z \approx 2$  and falls off at high redshift. If, as suggested by Pettini et al. (1998) and Steidel et al. (1999), there is little or no falloff in the star formation rate out to  $z \approx 4$ , the mean intensity at  $z = 0$  would increase by only 10%. This is a small effect because of redshifting and the fact that stars emit few photons more energetic than 4 rydbergs. Thus, stars at  $z > 3$  would make little contribution to  $I_0$  at  $z = 0$ . Also, because stellar radiation does not doubly ionize He, diffuse He II

Ly $\alpha$  and two-photon emission from absorbers make little contribution to  $I_0$  at  $z = 0$ .

#### 4. CONCLUSIONS

In this paper, we have endeavored to make accurate estimates of the low-redshift intensity of ionizing radiation, arising from QSOs, Seyfert galaxies, and starburst galaxies. In performing this calculation, we found that we require accurate values of AGN emissivity and IGM opacity out to substantial redshifts. In other words, this is a global problem.

Our new estimates of the ionizing emissivities of Seyfert galaxies and low-redshift QSOs were constructed by extrapolating ultraviolet fluxes from IUE to the Lyman limit. For starburst galaxies, we used recent H $\alpha$  surveys together with an educated guess for the escaping fraction of ionizing radiation. The IGM opacity was derived from HST surveys of the low-redshift Ly $\alpha$  absorbers and a new opacity model from *Keck* high-resolution spectra of high-redshift QSOs. By incorporating these ingredients into a cosmological radiative transfer code, we find that the ionizing intensity at  $z \approx 0$  has approximately equal contributions from AGN and starburst galaxies:

$$I_0^{\text{AGN}} = (1.3 \times 10^{-23} \text{ erg cm}^{-2} \text{ s}^{-1} \text{ Hz}^{-1} \text{ sr}^{-1}) \left[ \frac{L_{\text{min}}}{0.01L_*} \right]^{-0.17} \left[ \frac{\alpha_s}{1.8} \right]^{-0.97} \quad (14)$$

$$I_0^{\text{Star}} = (1.1 \times 10^{-23} \text{ erg cm}^{-2} \text{ s}^{-1} \text{ Hz}^{-1} \text{ sr}^{-1}) \left[ \frac{\langle f_{\text{esc}} \rangle}{0.05} \right] \left[ \frac{L_{\text{H}\alpha}}{10^{39.1}} \right] \quad (15)$$

Taking into account uncertainties in the various parameters of the model ( $L_{\text{min}}$ ,  $\alpha_s$ , QSO luminosity function, H $\alpha$ -determined star-formation history) we estimate uncertainties in these coefficients of  $1.3_{-0.5}^{+0.8}$  (for AGN) and  $1.1_{-0.7}^{+1.4}$  (for starbursts). For a spectral index  $\alpha_s \approx 1.8$  (from 1 – 4 Ryd), these values of  $I_0$  each correspond to one-sided ionizing fluxes  $\Phi_{\text{ion}} \approx 3000 \text{ photons cm}^{-2} \text{ s}^{-1}$ . Allowing for statistical uncertainties, the total ionizing photon flux at low redshift probably lies in the range  $\Phi_{\text{ion}} = 2000 - 10,000 \text{ photons cm}^{-2} \text{ s}^{-1}$ , which is consistent with a number of recent estimates and measurements (see Table 1).

The redshift evolution of the hydrogen photoionization rate,  $\Gamma_{\text{HI}}(z)$  is shown in Figure 9 for three cases: AGN only, starbursts only, and combined (AGN plus starbursts). These rates were computed using our standard emissivity models for AGN and starburst galaxies, except that the starburst emissivities were held constant at  $z > 1.7$  to simulate recent measurements at high  $z$ . The starburst emissivities also assume  $\langle f_{\text{esc}} \rangle = 0.05$ . Although it is beyond the scope of this paper, the potentially dominant role of starburst galaxies in photoionization at  $z > 4$  is apparent.

Because the values in eqs. (14) and (15) include unacceptably large range for such an important quantity, it is worth discussing what might be done to improve the situation, both theoretically and observationally. Advances need to be made in the characterization of both ionizing emissivities and IGM opacities. The greatest uncertainty in the opacity model occurs in the range  $\log N_{\text{HI}} = 15 - 17$ , where line saturation and small-number statistics make the Ly $\alpha$

surveys inaccurate. The imminent launch of the FUSE satellite will open up the far-UV band (920–1180 Å) that contains Ly $\beta$  and higher Lyman series lines. A survey of Ly $\beta$  lines should allow better determinations of line saturation (doppler  $b$ -values). The FUSE spectra of AGN will also provide more accurate values of the flux near the Lyman limit and reduce the uncertainties introduced by extrapolating from spectral regions longward of 1200 Å, as we have done with IUE data.

To address the general problem of small-number statistics in the Ly $\alpha$  absorbers, the HST Cosmic Origins Spectrograph (Morse et al. 1998), scheduled for installation on HST in 2003, should be used for a QSO absorption-line key project. A full discussion of the advantages of this project is given in Appendix 1 of the UV-Optical Working Group White Paper (Shull et al. 1999). Because COS will have about 20 times the far-UV throughput of the previous HST spectrographs, GHRS and STIS, and offers velocity resolution 10 times better than that of FOS, it will provide much better statistics on the distribution of H I absorbers in both space and column density. The most useful COS surveys will be of low-redshift Ly $\alpha$  lines, particularly the rare “partial Lyman-limit systems” ( $16.0 < \log N_{HI} < 17.5$ ). Accurately characterizing the distribution in column density and the evolution in redshift of these absorbers would remove a large part of the uncertainty in the IGM opacity model.

The emissivity models for both AGN and starburst galaxies also need improvement. Although we have used current surveys of Seyfert galaxies and QSOs, we may have missed certain classes of sources that are strong emitters in the EUV. We believe that BL Lac objects contribute less than 10% of Seyferts, based on estimates of their luminosity function and space density. On the other hand, Edelson et al. (1999) suggest that narrow-line Seyfert 1 galaxies may account for  $\sim 50\%$  of the EUV volume emissivity in the ROSAT Wide-Field Camera sample. It is not clear whether these Seyferts are captured in the Cheng et al. (1985) luminosity function, but their ionizing spectra might be higher than that derived from an extrapolation of their UV fluxes. For low-redshift starbursts, two recent surveys (Gallego et al. 1995; Gronwall 1998) derive comparable values of H $\alpha$  luminosity density, although even the latter (KISS) H $\alpha$  survey may still be incomplete at the faint end. At higher redshifts, the QSO luminosity function is uncertain, owing to the effects of dust (Fall & Pei 1993; Pei 1995) and faint-end survey incompleteness. QSO surveys by GALEX (Galaxy Explorer) in the ultraviolet and by the Sloan Digital Sky Survey in the optical may clarify the AGN luminosity functions. However, it is worth repeating that, owing to redshifting and IGM opacity, AGN and starbursts at  $z > 3$  contribute less than 10% to the value of  $I_0$  at  $z = 0$ .

For an accurate emissivity density, what is needed most are surveys at  $z < 1$  of AGN and starburst galaxies. Even after we ascertain the space density and H $\alpha$  luminosity functions of star-forming galaxies, we still need an accurate measurement of  $\langle f_{\text{esc}} \rangle$ , the fraction of stellar ionizing photons that escape the galactic H I layers into the halo and IGM. Here, we have relied on recent theoretical work (Dove et al. 1999) and H $\alpha$  observations of gas in the Magellanic Stream (Bland-Hawthorn & Maloney 1999) that suggest  $\langle f_{\text{esc}} \rangle \approx 0.03 - 0.06$ . However, access with FUSE to the far-UV spectrum at 920–950 Å allows a direct measurement of the escaping



EUV continuum from starbursts at redshifts  $z \approx 0.05$ . This work will extend the studies with the Hopkins Ultraviolet Telescope (HUT) of leaky starbursts (Leitherer et al. 1995; Hurwitz et al. 1997).

Finally, we eagerly await new measurements of the ionizing photon flux,  $\Phi_{\text{ion}}$  via several direct and indirect techniques. These methods include improved Fabry-Perot measurements of  $\text{H}\alpha$  from Galactic high-velocity clouds (Tuftte et al. 1998; Bland-Hawthorn & Maloney 1999), and UV absorption-line measurements of ionization ratios such as Fe I/Fe II and Mg I/Mg II that constrain the far-UV radiation in the 0.6–1.0 Ryd band (Stocke et al. 1991; Tumlinson et al. 1999). A new absorption-line key project with HST/COS could make precise estimates of  $I_0$  from the proximity effect. As a result of the new surveys and ventures mentioned above, it should be possible, within five years, to determine the local ionizing background to  $< 30\%$ . With good fortune, these measurements and the theoretical models will agree to a level better than described here in Table 1.

This work was supported by theoretical grants from NASA (NAG5-7262) and NSF (AST96-17073). The IUE spectral analysis was supported by a grant from NASA’s Astrophysical Data Program (NAG5-3006).

**Table 1**  
**Measurements and Limits of low- $z$  Ionizing Background<sup>1</sup>**

Technique	$\Phi_{\text{ion}}$ ( $\text{cm}^{-2} \text{s}^{-1}$ )	Reference
H $\alpha$ Fabry-Perot	$< 3 \times 10^4$	Vogel et al. (1995)
H $\alpha$ Filter Images	$< 1.1 \times 10^4$	Donahue et al. (1995)
H $\alpha$ Filter Images	$< 8.4 \times 10^4$	Stocke et al. (1991)
H $\alpha$ Filter Images	$< 9 \times 10^4$	Kutyrev & Reynolds (1989)
H I Disk Edges	$(0.5 - 5) \times 10^4$	Maloney (1993)
H I Disk Edges	$(1 - 5) \times 10^4$	Dove & Shull (1994a)
Prox. Eff. $\langle z \rangle = 0.5$	$(0.05 - 1.0) \times 10^4$	Kulkarni & Fall (1993)

<sup>1</sup>  $\Phi_{\text{ion}}$  is the one-sided, normally incident photon flux in the metagalactic background, related to the specific intensity at Lyman limit by  $\Phi_{\text{ion}} = (2630 \text{ cm}^{-2} \text{ s}^{-1}) I_{-23}(1.8/\alpha_s)$  – see eq. (1) in text.

**Table 2**  
**Low- $z$  Opacity Models**

Model	$N_{\text{min}}(\text{cm}^{-2})$	$N_{\text{max}}(\text{cm}^{-2})$	$A_i$	$\beta_i$	$\gamma_i$	$c_i$	$s_i$
Standard	...	$10^{14}$	0.105	1.63	0.15	0.010	-2.81
	$10^{14}$	$10^{17}$	0.501	1.50	0.15	0.553	-2.73
	$10^{17}$	$10^{22}$	0.159	1.50	1.5	0.263	-1.04
Model 1	...	$10^{15.5}$	0.105	1.63	0.15	0.048	-2.81
	$10^{15.5}$	$10^{22}$	0.159	1.50	1.5	0.411	-1.38
Model 2	...	$10^{15.5}$	0.105	1.63	0.15	0.048	-2.81
	$10^{17}$	$10^{22}$	0.159	1.50	1.5	0.263	-1.04

## REFERENCES

- Bahcall, J. N., Jannuzi, B. T., Schneider, D. P., Hartig, G. F., Bohlin, R., & Junkkarinen, V. 1991, *ApJ*, 377, L5
- Bajtlik, S., Duncan, R. C., & Ostriker, J. P. 1988, *ApJ*, 327, 570
- Barger, A. J., et al. 1998, *Nature*, 394, 248
- Bechtold, J., Weymann, R. J., Lin, Z., & Malkan, M. 1987, *ApJ*, 315, 180
- Bland-Hawthorn, J. & Maloney, P. 1999, *ApJ*, 510, L33
- Bland-Hawthorn, J., Taylor, K., Veilleux, S., & Shopbell, P. L. 1994, *ApJ*, 437, L95
- Boyle, B. J. 1993, in *The Environment and Evolution of Galaxies*, eds. J. M. Shull & H. A. Thronson, (Dordrecht: Kluwer), 433
- Cheng, F.-Z., Danese, L., De Zotti, G., & Franceschini, A. 1985, *MNRAS*, 212, 857
- Connolly, A. J., Szalay, A. S., Dickinson, M., SubbaRao, M. U., & Brunner, R. J. 1997, *ApJ*, 486, L11
- Cooke, A. J., Espey, B., & Carswell, B. 1997, *MNRAS*, 284, 552
- Davé, R., Hernquist, L., Katz, N., & Weinberg, D. H. 1999, *ApJ*, 511, 521
- Deharveng, J.-M., Faisse, S., Milliard, B. & Le Brun, V. 1997, *A&A*, 325, 1259
- Della Ceca, R., Zamorani, G., Maccacaro, T., Setti, G., & Wolter, A. 1996, *ApJ*, 465, 650
- Donahue, M., Aldering, G., & Stocke, J. T. 1995, *ApJ*, 450, L45
- Dove, J. B., & Shull, J. M. 1994a, *ApJ*, 423, 196
- Dove, J. B., & Shull, J. M. 1994b, *ApJ*, 430, 222
- Dove, J. B., Shull, J. M., & Ferrara, A. 1999, *ApJ*, submitted (astro-ph/9903331)
- Edelson, R., Vaughan, S., Warwick, R., Puchnarewicz, E., & George, I. 1999, *MNRAS*, in press (astro-ph/9903198)
- Efstathiou, G. 1992, *MNRAS*, 256, 43
- Fall, S. M., & Pei, Y. 1993, *ApJ*, 402, 479
- Fardal, M. A., & Shull, J. M. 1993, *ApJ*, 415, 524
- Fardal, M. A., Giroux, M. L., & Shull, J. M. 1998, *AJ*, 115, 2206 (FGS)
- Gallego, J., Zamorano, J., Aragon-Salamanca, A. & Rego, M. 1995, *ApJ*, 455, L1
- Giallongo, E., Fontana, A., & Madau, P. 1997, *MNRAS*, 289, 629
- Giallongo, E., Cristiani, S., D’Odorico, S., Fontana, A., & Savaglio, S. 1996, *ApJ*, 466, 46
- Goldschmidt, P., & Miller, L. 1998, *MNRAS*, 293, 107
- Goldschmidt, P., Miller, L., La Franca, F. & Cristiani, S. 1992, *MNRAS*, 256, 65

- Gronwall, C. 1998, to appear in Dwarf Galaxies and Cosmology, ed. T. Thuan, et al., Editions Frontières, astro-ph/9806240
- Gronwall, C., Salzer, J. J., & McKinsty, K. 1998, BAAS, 30, 1369
- Haardt, F., & Madau, P. 1996, ApJ, 461, 20
- Heisler, J. & Ostriker, J. P. 1988, ApJ, 332, 543
- Hughes, D. H., et al. 1998, Nature, 394, 241
- Hurwitz, M., Jelinsky, P. & Dixon, W. V. D. 1997, ApJ, 481, L31
- Hurwitz, M. et al. 1998, ApJ, 500, L61
- Ikeuchi, S., & Turner, E. L. 1991, ApJ, 381, L1
- Januzzi, B. et al. 1998, ApJS, 118, 1
- Köhler, T., Groote, D., Reimers, D., & Wisotzki, L. 1997, A&A, 325, 502
- Kulkarni, V. P., & Fall, S. M. 1993, ApJ, 413, L63
- Kutyrev, A. S., & Reynolds, R. J. 1989, ApJ, 344, L9
- La Franca, F. & Cristiani, S. 1997, AJ, 113, 1517
- Leitherer, C., Ferguson, H. C., Heckman, T. M., Lowenthal, J. D. 1995, ApJ, 454, L19
- Madau, P. 1992, ApJ, 389, L1
- Madau, P. 1998, in The Birth of Galaxies, proceedings of 10<sup>th</sup> Recontres de Blois, eds. B. Guideroni et al., Editions Frontières, astro-ph/9812087
- Madau, P., & Shull, J. M. 1996, ApJ, 457, 551
- Maloney, P. 1993, ApJ, 414, 41
- Miralda-Escudé, J., & Ostriker, J. P. 1990, ApJ, 350, 1
- Morris, S. L., Weymann, R. J., Savage, B. D., & Gilliland, R. L. 1991, ApJ, 377, L21
- Morse, J. A., Green, J. C., et al. 1998, Proc. SPIE, 3356, 361
- Paresce, F., McKee, C. F., & Bowyer, S. 1980, ApJ, 240, 387
- Peebles, P. J. E. 1993, Physical Cosmology, Princeton Univ. Press
- Pei, Y.-C. 1995, ApJ, 438, 623
- Penton, S. V., Shull, J. M., & Edelson, R. 1996, Database of IUE-AGN Ultraviolet Spectra, available on <http://casa.colorado.edu/~spenton/IUEAGN/FUSE.html>
- Penton, S. V., Stocke, J. T., & Shull, J. M. 1999, in preparation
- Petitjean, P., Webb, J. K., Rauch, M., Carswell, R. F., & Lanzetta, K. 1993, MNRAS, 262, 499
- Pettini, M. et al. 1998, *Origins*, ed. C. E. Woodward, J. M. Shull, & H. Thronson (ASP Conference Series vol. 148), 67

- Quinn, T., Katz, N., & Efstathiou, G. 1996, MNRAS, 278, L49
- Sandage, A. 1973, ApJ, 180, 687
- Schmidt, M., & Green, R. F. 1983, ApJ, 269, 352
- Scott, J., Bechtold, J., Dobrzycki, A., & Kulkarni, V. 1999, BAAS, 1336
- Shull, J. M. 1997, in Structure and Evolution of the Intergalactic Medium from QSO Absorption Line Systems, ed. P. Petitjean, S. Charlot (Paris: Edition Frontières), 101
- Shull, J. M., Penton, S. V., Stocke, J. T. 1999, Publ. Astr. Soc. Australia, 16, No. 1, 95 (astro-ph/9901280)
- Shull, J. M., Penton, S. V., Stocke, J. T., Giroux, M. L., van Gorkom, J. H., Lee, Y.-H., & Carilli, C. 1998, AJ, 116, 2206
- Shull, J. M., Savage, B. D., Morse, J. A., et al. 1999, The Emergence of the Modern Universe: Tracing the Cosmic Web, report of NASA UV-Optical Working Group, in press, available on <http://casa.colorado.edu/~uvconf/UVOWG.html>.
- Stocke, J. T., Case, J., Donahue, M., Shull, J. M., & Snow, T. P. 1991, ApJ, 374, 72
- Steidel, C. C., Adelberger, K. L., Dickinson, M., Giavalisco, M., & Pettini, M. 1999, ApJ, 519, 1
- Storrie-Lombardi, L. J., McMahon, R. G., Irwin, M. J., & Hazard, C. 1994, ApJ, 427, L13
- Stengler-Larrea, E. A. et al. 1995, ApJ, 444, 64
- Theuns, T., Leonard, A., & Efstathiou, G. 1998, MNRAS, 297, L49
- Tufte, S. L., Reynolds, R. J., & Haffner, L. M. 1998, ApJ, 504, 773
- Tumlinson, J., Giroux, M. L., Shull, J. M., & Stocke, J. T. 1999, submitted to AJ
- Vogel, S. N., Weymann, R., Rauch, M., & Hamilton, T. 1995, ApJ, 441, 162
- Weedman, D. 1986, Quasar Astronomy, Cambridge Univ. Press
- Weymann, R. J. et al. 1998, ApJ, 506, 1
- Yee, H. K. C., 1983, ApJ, 272, 473
- Zheng, W., Kriss, G. A., Telfer, R. C., Grimes, J. P., & Davidsen, A. F. 1997, ApJ, 475, 469

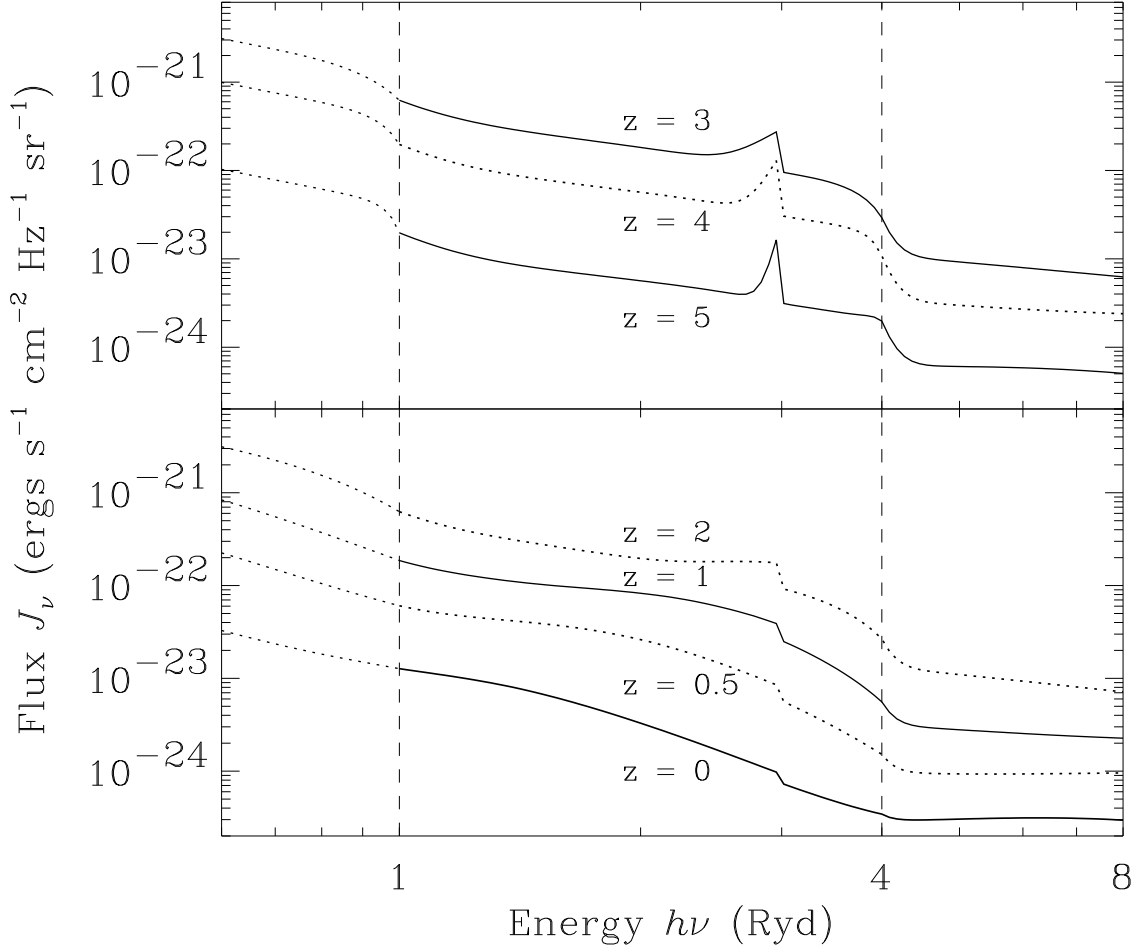


Fig. 1.— Evolution of the ionizing background with redshift, assuming the modified Pei luminosity function for AGN described in § 2.1 ( $\Omega_0 = 0.2, h = 0.5, \alpha_{UV} = 0.86, \alpha_s = 1.8$ ). The opacity is a hybrid model consisting of Model A2 from FGS for  $z > 1.9$ , and our standard model for the low redshift opacity for  $z < 1.9$ . This calculation incorporates the full radiative transfer and reradiation of ionizing photons by absorbers described in FGS. Top panel:  $3 \leq z \leq 5$ . Bottom panel:  $0 \leq z \leq 2$ .

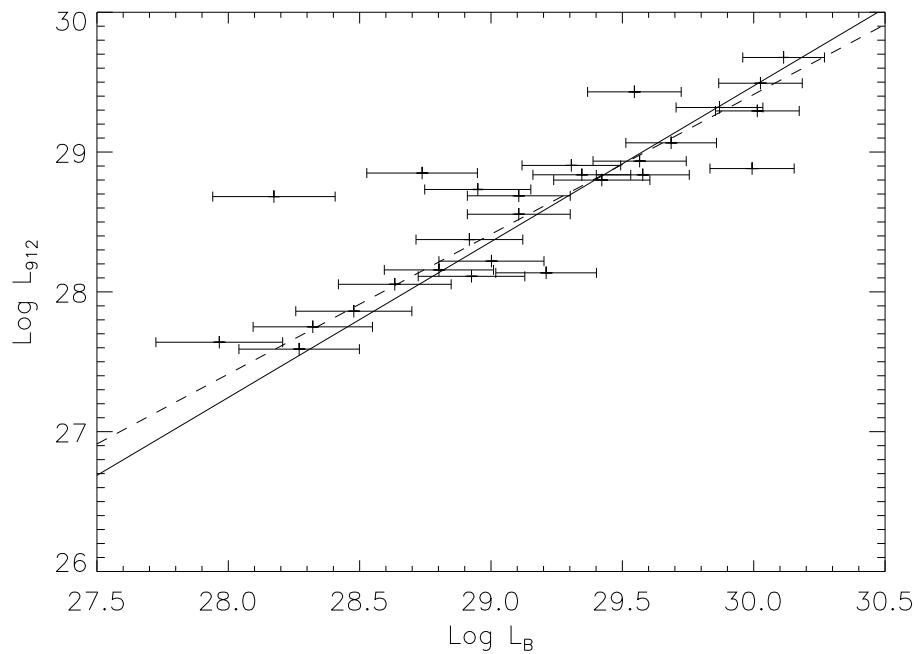


Fig. 2.— Correlation between  $L_{912}$  and  $L_B$  for the 27 Seyferts in our subsample. A least-squares fit gives a slope of  $1.114 \pm 0.081$  with  $\chi^2 = 65.5$ . For comparison, the dashed curve shows a constant optical spectral index of  $\alpha_{UV} = 0.86$  between  $4400 \text{ \AA}$  and  $912 \text{ \AA}$ .

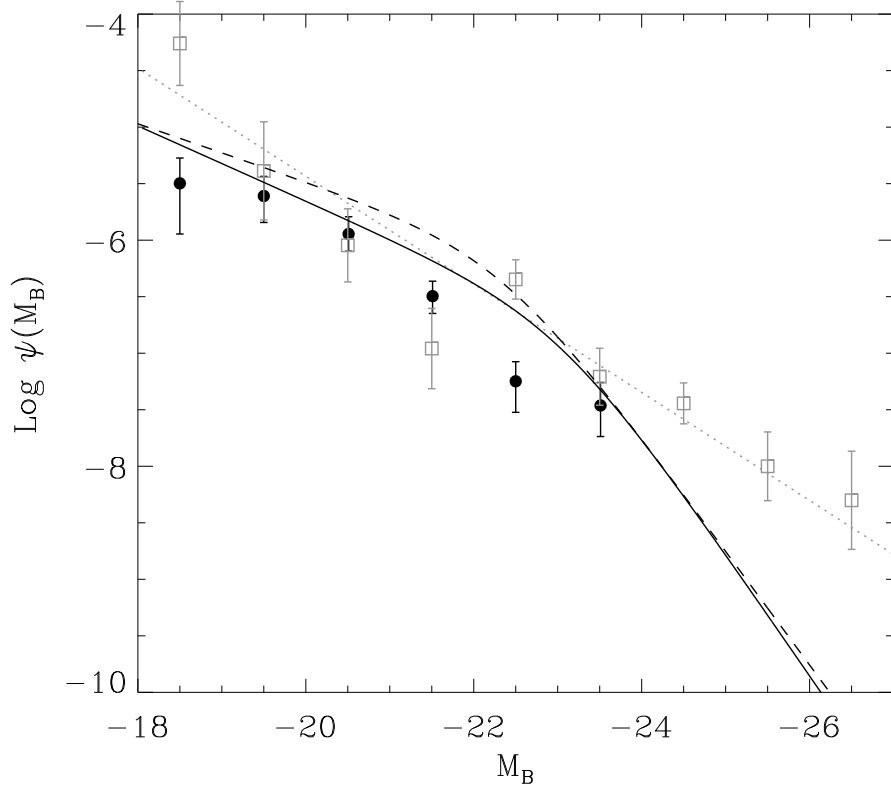


Fig. 3.— AGN luminosity functions. Circles show the Seyfert galaxy sample of Cheng et al. (1995) from which the 27 Seyfert galaxies in common with our IUE-AGN database (Penton et al. 1998) were taken (see Fig. 2). Squares show the Seyfert galaxy sample of Köhler et al. (1997), and dotted curve represents a power law fit  $\Phi(L_B) \propto L_B^{-2.2}$  to these latter results. The solid and dashed curves are an extrapolation to  $z = 0$  of the Pei (1995) luminosity function for  $h = 0.5, \Omega_0 = 0.2$  and  $h = 0.5, \Omega_0 = 1$ , respectively. Note that at  $z = 0$ , the AGN fitted by Pei only went down to  $0.7L_*$  corresponding to  $M_B = -23.5$ .



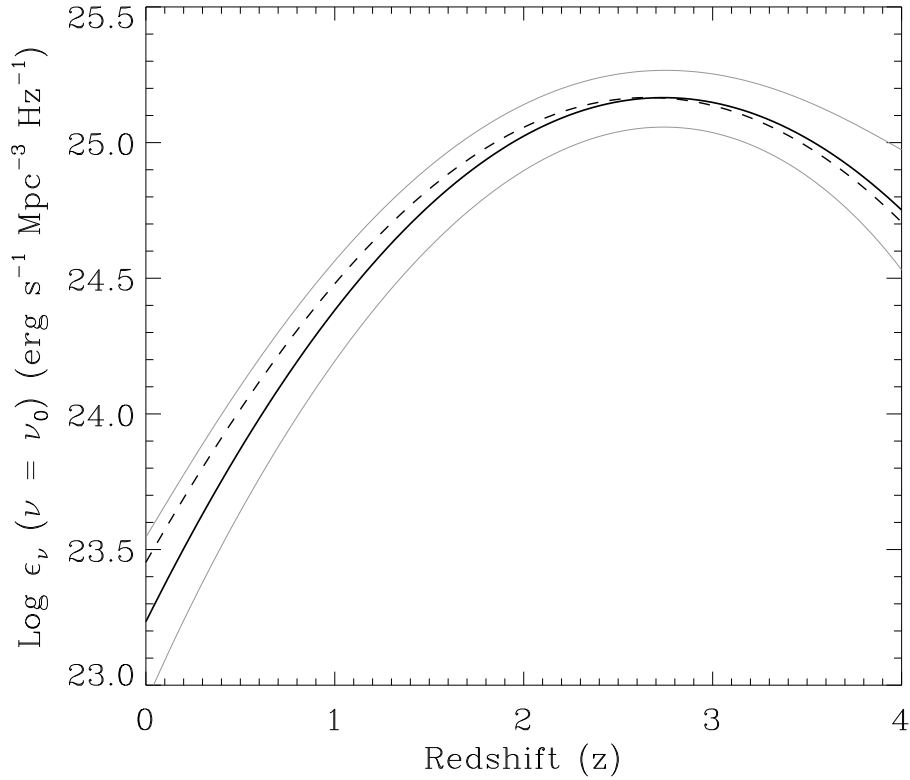


Fig. 4.— Source emissivity due to AGN at redshift  $z$  for modified Pei open model ( $\Omega_0 = 0.2$ ,  $h = 0.5$ , and  $\alpha_{\text{UV}} = 0.86$ ) (solid curve) and modified Pei closed model ( $\Omega_0 = 1$ ,  $h = 0.5$ , and  $\alpha_{\text{UV}} = 0.86$ ; correction for open universe line element) (dashed curve). Dotted curves frame our  $1\sigma$  range in emissivity for the open model, including corrections for completeness of the luminosity function, and a variation of the  $L_{912}/L_B$  ratio by one standard deviation in spectral slope and dependence on  $L_B$ .

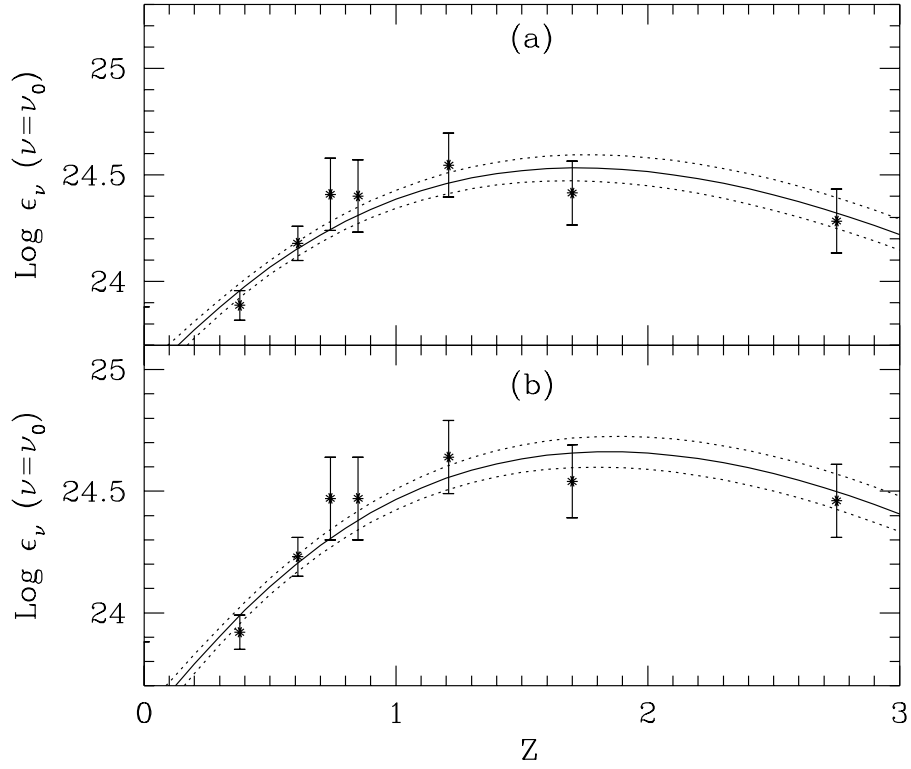


Fig. 5.— (a) Source emissivity due to galaxies at redshift  $z$ , tied to Gallego et al. (1995) and Connolly et al. (1997). Assumes  $\Omega_0 = 0.2$ ,  $h = 0.5$ , and  $\langle f_{esc} \rangle = 0.05$ ,  $T = 2 \times 10^4$  K,  $\langle h\nu \rangle = 22$  eV. Dotted curves frame our  $1\sigma$  range in emissivity. (b) Same as (a), except  $\Omega_0 = 1$

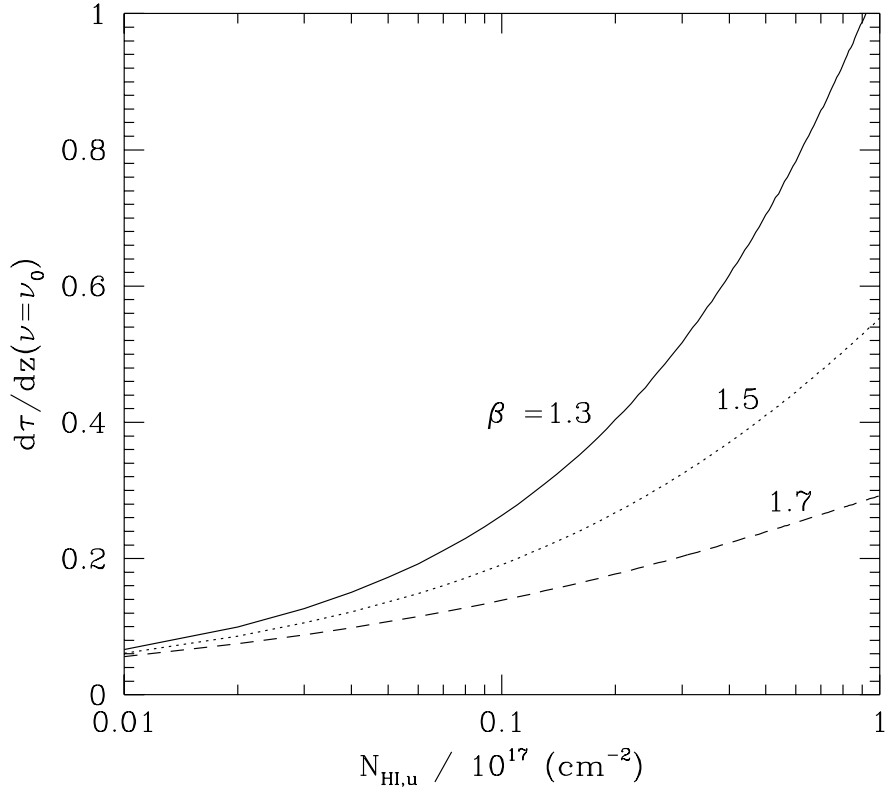


Fig. 6.— Differential continuum opacity,  $d\tau_{\text{eff}}/dz$ , at  $\nu = \nu_0$  and  $z = 0$ , versus the assumed upper limit on the column density distribution. We consider HST/FOS sample 5 of Weymann et al. (1998) of 465 Ly $\alpha$  absorbers with  $W_\lambda > 240$  mÅ, for which  $dN/dz = 30.7 \pm 4.2$ . We model these lines as a distribution,  $N_{HI}^{-\beta}$ , of column densities from  $N_{HI} = 10^{14}$  cm $^{-2}$  up to  $N_{HI,u}$ . In ascending order, these curves assume  $\beta = 1.7$ , 1.5, and 1.3.

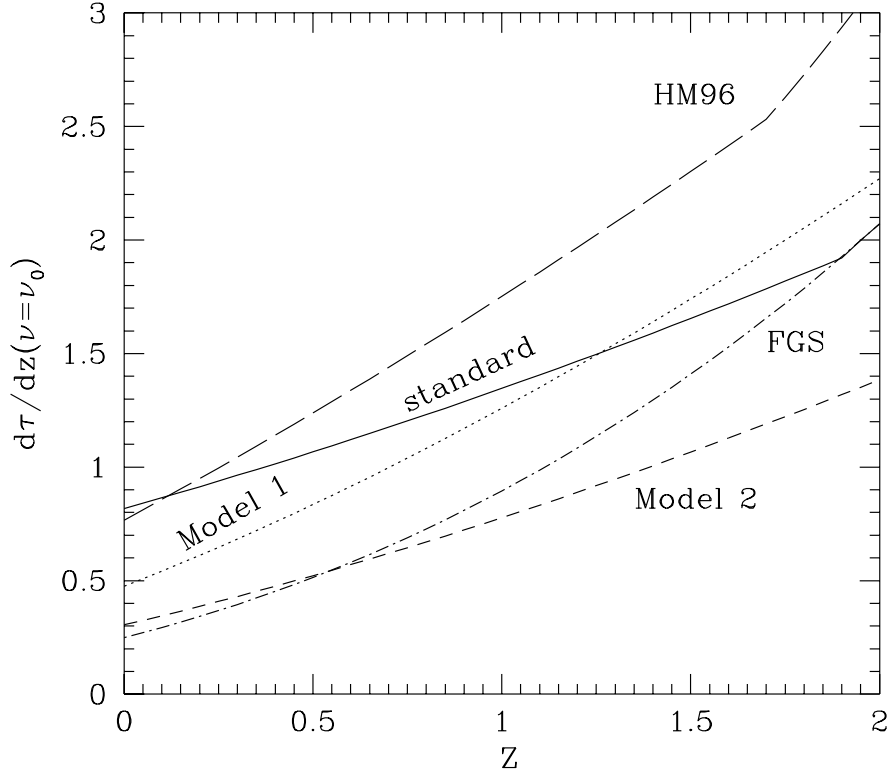


Fig. 7.— Differential continuum opacity,  $d\tau_{\text{eff}}/dz$ , at  $\nu = \nu_0$  versus redshift  $z$  for models for the column density distribution of Ly $\alpha$  forest and Lyman limit systems. Solid curve is our “standard model” described in Table 2. Dotted curve is our Model 1, and short-dashed curve is our model 2. Dot-dashed curve is the extrapolation to low  $z$  of Model A2 from FGS. Long-dashed curve is the opacity assumed by Haardt & Madau (1996).

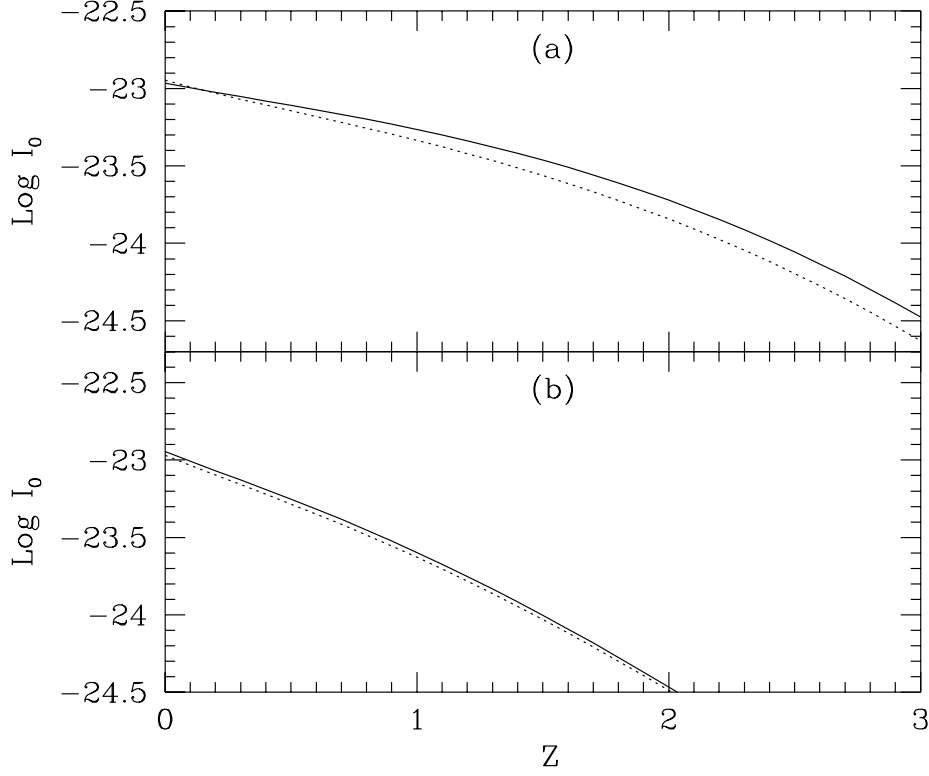


Fig. 8.— (a) Cumulative value of  $I_0(z = 0)$  arising from AGN at redshifts greater than  $z$ . These intensities are calculated using the approximate method (eqs. (3-5]) that neglects diffuse ionizing radiation from the absorbers. Solid curve assumes  $\Omega_0 = 0.2, h = 0.5$ ; dotted curve assumes  $\Omega_0 = 1, h = 0.5$ . Standard model for opacity is used for both. At  $z = 0$ ,  $I_0 = 1.09 \times 10^{-23}$  and  $I_0 = 1.13 \times 10^{-23}$  for these respective cases. (b) Cumulative value of  $I_0$  arising from galaxies at redshift  $z$ , assuming  $\Omega_0 = 0.2, h = 0.5$ , (solid curve) or  $\Omega_0 = 1, h = 0.5$ , (dotted curve),  $\langle f_{esc} \rangle = 0.05$ , and standard model for opacity. At  $z = 0$ ,  $I_0 = 1.13 \times 10^{-23}$  and  $I_0 = 1.07 \times 10^{-23}$  for the respective cases.

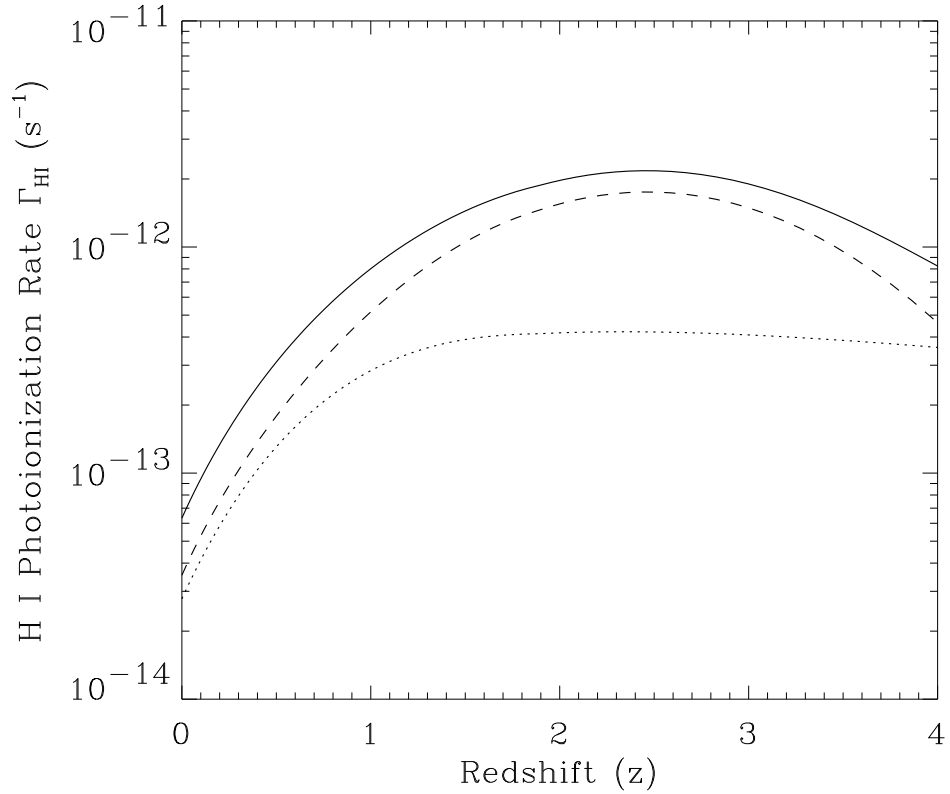


Fig. 9.— Hydrogen photoionization rate versus redshift for three cases: AGN-only (dashed curve), starburst galaxies only (dotted), and combined (solid curve). Each case assumes the standard models for emissivity (§ 2.1, 2.2) and opacity (§2.3 and Fig. 1 caption). The AGN emissivities are the same as solid curve in Fig. 4, while starburst emissivities are same as solid curve in Fig. 5a, except that the comoving emissivity is held constant for  $1.7 < z < 4.0$  to simulate recent measurements of star-formation history.